Ontogeny of Head and Caudal Fin Shape of an Apex Marine Predator: The Tiger Shark (*Galeocerdo Cuvier*)

Amy L. Fu,[1] Neil Hammerschlag,[2,3,4] George V. Lauder,[5] Cheryl D. Wilga,[6] Chi-Yun Kuo,[7] and Duncan J. Irschick[1,7]*

[1]*Department of Biology, 221 Morrill Science Center, University of Massachusetts at Amherst, Amherst, Massachusetts 01003*
[2]*Rosenstiel School of Marine and Atmospheric Science, University of Miami, Miami, Florida*
[3]*Leonard and Jayne Abess Center for Ecosystem Science and Policy, University of Miami, Coral Gables, Florida*
[4]*Shark Research and Conservation Program, University of Miami, Miami, Florida*
[5]*Museum of Comparative Zoology, Harvard University, Cambridge, Massachusetts 02138*
[6]*Department of Biological Sciences, University of Rhode Island, Kingston, Rhode Island 02881*
[7]*Organismic and Evolutionary Biology Program, University of Massachusetts, Amherst, Massachusetts 01003*

ABSTRACT How morphology changes with size can have profound effects on the life history and ecology of an animal. For apex predators that can impact higher level ecosystem processes, such changes may have consequences for other species. Tiger sharks (*Galeocerdo cuvier*) are an apex predator in tropical seas, and, as adults, are highly migratory. However, little is known about ontogenetic changes in their body form, especially in relation to two aspects of shape that influence locomotion (caudal fin) and feeding (head shape). We captured digital images of the heads and caudal fins of live tiger sharks from Southern Florida and the Bahamas ranging in body size (hence age), and quantified shape of each using elliptical Fourier analysis. This revealed changes in the shape of the head and caudal fin of tiger sharks across ontogeny. Smaller juvenile tiger sharks show an asymmetrical tail with the dorsal (upper) lobe being substantially larger than the ventral (lower) lobe, and transition to more symmetrical tail in larger adults, although the upper lobe remains relatively larger in adults. The heads of juvenile tiger sharks are more conical, which transition to relatively broader heads over ontogeny. We interpret these changes as a result of two ecological transitions. First, adult tiger sharks can undertake extensive migrations and a more symmetrical tail could be more efficient for swimming longer distances, although we did not test this possibility. Second, adult tiger sharks expand their diet to consume larger and more diverse prey with age (turtles, mammals, and elasmobranchs), which requires substantially greater bite area and force to process. In contrast, juvenile tiger sharks consume smaller prey, such as fishes, crustaceans, and invertebrates. Our data reveal significant morphological shifts in an apex predator, which could have effects for other species that tiger sharks consume and interact with. J. Morphol. 277:556–564, 2016.   © 2016 Wiley Periodicals, Inc.

KEY WORDS: sharks; morphology; ontogeny; ecology; form

INTRODUCTION

As organisms mature, they often undergo ecological transitions in both movement patterns and diet, among other changes (Calder, 1984; Werner and Gillam, 1984; Schmidt-Nielsen, 1984; Wainwright et al., 1991; Eggold and Motta, 1992; Carrier, 1996; Tyler-Bonner and Horn, 2000). For example, many fish species transition from being relatively sedentary in shallow nursery areas to more mobile once they mature and leave the nursery for the open ocean (Beck et al., 2001). Dietary shifts are also common in animals, such as ontogenetic changes in diet from insectivory to herbivory in lizards (Herrel et al., 2004), or between soft and hard prey in fish (Alfaro et al., 2005). Such ecological shifts are often accompanied by notable changes in body shape as animals' age (LaBarbera, 1989; Carrier, 1996). For apex predators that can have profound effects on other ecosystem processes (Estes et al., 2011), ontogenetic changes in ecology and body shape can have substantial

impacts on other species, especially those they directly prey on.

Tiger sharks (*Galeocerdo cuvier*) are generalist apex predators in temperate and tropical seas (Cortes, 1999; Heithaus, 2001; Compagno et al., 2005). They are highly migratory, linking disparate habitats (e.g., Heithaus et al., 2007; Fitzpatrick et al., 2012; Papastamatiou et al., 2013; Ferriera et al., 2015; Hammerschlag et al., 2012). Whereas juvenile tiger sharks are able to make long-distance migrations, they exhibit more circumscribed movements than adults do (e.g., Werry et al., 2014; Alfonso and Hazin, 2015; Lea et al., 2015), although around Hawaii, juvenile tiger sharks appear to be more wide ranging than adult females (Meyer et al. 2009). Tiger sharks have a diverse diet, but undergo an ontogenetic diet expansion with age (Lowe et al., 1996; Cortes, 1999; Simpfendorfer et al., 2001, Heithaus, 2001). As juveniles, tiger sharks consume primarily fish, crustaceans, and other organisms, whereas as adults their diet expands to also include larger and harder prey, such as sea turtles, marine mammals, and other sharks (Lowe et al., 1996; Cortes, 1999; Simpfendorfer et al., 2001; Heithaus, 2001). These two ontogenetic ecological shifts (changes in overall migration patterns and harder prey size and rigidity) may be accompanied by changes in body shape as tiger sharks mature.

Sharks, like other fishes (Thomson and Simanek 1977; Webb 1984; Lauder, 2000; Lauder et al., 2003; Blake, 2004), exhibit wide variation in caudal fin shape (Thomson and Simanek, 1977; Ferry and Lauder, 1996; Wilga and Lauder, 2002, 2004a,b; Flammang et al., 2011). In general, high-performance sharks, such as some laminid species (e.g., white sharks, *Carcharodon carcharias*, mako sharks, *Isurus*) tend to have stiff symmetrical tails that may allow them to produce higher thrust forces, and therefore swim at faster speeds (Lingham-Soliar, 2005a,b). On the other extreme, slower moving sharks, such as nurse (*Ginglystoma cirratum*) or some cow sharks (Hexanchidae) exhibit more compliant and asymmetrical tails in which the upper lobe is substantially longer than the lower lobe (Thomson and Simanek, 1977; Wilga and Lauder, 2004a; Reiss and Bonnan, 2010).

Prior theoretical and empirical work suggests that stiff symmetrical tails are suited for open-water fast cruising whereas compliant, asymmetrical tails are better suited for slower swimming or maneuvering in complex environments (Thomson and Simanek, 1977; Wilga and Lauder, 2004a). However, there has been little analysis of whether similar transitions also occur intra-specifically among ontogenetic classes within a shark species. In general, the available data for smaller shark species, such as spiny dogfish (*Squalus acanthias*), blacktip (*Carcharhinus limbatus*), and nurse sharks (*Ginglymostoma cirratum*) show isometric changes in the caudal fin as they age (Reiss and Bonnan, 2010; Irschick and Hammerschlag, 2014), whereas in larger apex shark species, such as white (*Carcharodon carcharias*), tiger (*Galeocerdo cuvier*), and bull sharks (*Carcharhinus leucas*), caudal fin area seems to scale with negative allometry (Lingham-Soliar, 2005a; Irschick and Hammerschlag, 2014). However, even among the larger species, these studies only examined either changes in area, or changes in length using linear morphometric measurements (e.g., length of the lower lobe of caudal fin), and did not examine overall shape changes of the caudal fin. Given that linear measures are not always representative of variation in shape, more data on how caudal fin shape can change with size is needed.

For tiger sharks, the transition from consuming generally smaller and softer prey in juveniles to larger and harder prey as adults could be linked with the potential for ontogenetic changes in head shape. Prior studies, mostly with terrestrial vertebrates, have generally shown that wider and deeper heads translate into stronger bites, although the dynamics of biting are complex, and depend on various factors, such as mechanical leverage and shear forces generated by teeth (Herrel et al., 1996; Huber et al., 2006, 2009; Habegger et al., 2012). Tiger sharks are unique among sharks in having a relatively broad head (in dorsal view), whereas most sharks have a more conical head shape that reduces drag (Lowe et al., 1996; Huber et al., 2006; Wirsing et al., 2006). The consumption of large hard prey such as adult sea turtles suggests that high bite forces and powerful jaws will be emphasized in adult tiger sharks, which may lead to corresponding shape changes in the head that enable increased bite area and force. Of course, other changes in the size, shape, and number of teeth, will also impact these parameters, as shown by Whitenack and Motta (2010) and Habegger et al. (2012), although we present no data on how these traits change with body size in tiger sharks. As body size and age are correlated within shark species (e.g., Casey et al., 1985; Casey and Natanson, 1992), we therefore have the opportunity to examine ontogenetic morphological changes in tiger sharks.

Accordingly, we set out to address two primary questions in tiger sharks. First, how does the shape and area of the caudal fin change with age? Second, how does the shape and area of the head, particularly for the dorsal side, change with age in tiger sharks? To address these questions, we collected data on 18 live tiger sharks captured and released in the Bahamas and Southern Florida varying more than threefold in length. Due to possible post-mortem changes in shape, using live animals for measurements of head and tail shape is preferable to using specimens in natural history collections. This could be especially true for
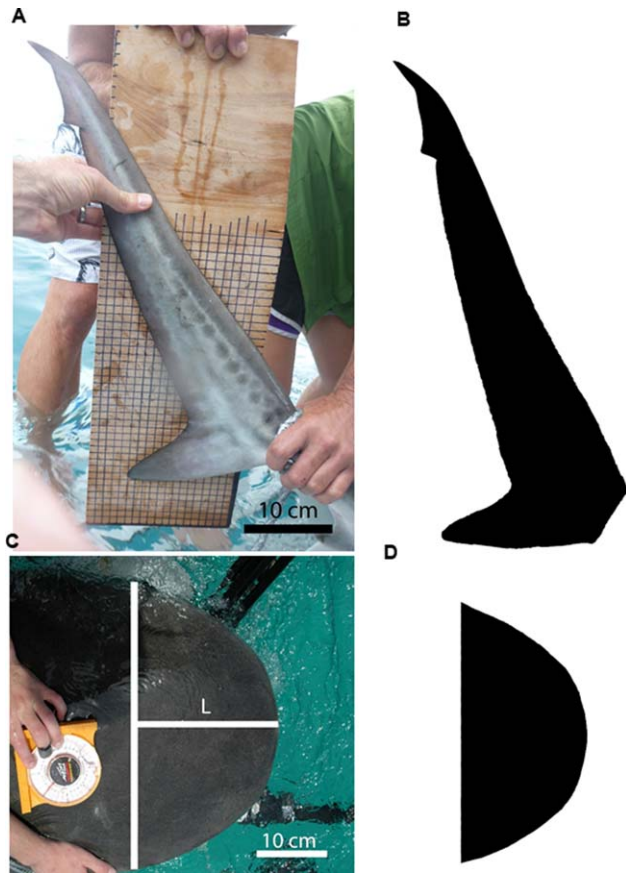
Fig. 1. (A) An image of a caudal fin used for area and shape measurements. (B) The same caudal fin shown in (A) but cut-out for measurement of area and shape. (C) An image of a tiger shark head taken from a dorsal view. (D) The same head image from (C) but cut-out for measurement of area and shape. [Color figure can be viewed in the online issue, which is available at wileyonlinelibrary.com.]

understanding relative proportions of tails and the head, which could be altered during preservation. We then used Elliptical Fourier Analysis (EFA) to quantify shape changes in the caudal fin and head as tiger sharks mature.

MATERIALS AND METHODS
Capturing Sharks

Tiger sharks were captured using standardized circle-hook drumlines (Gallagher et al., 2014). Briefly, drumlines were composed of a weighted base that sits on the seafloor. Attached to the weight was a 23-m monofilament line (400 kg test) that terminated in a baited 16/0 offset circle hook. The gear was left for 1 h before retrieval. When a tiger shark was captured, it was restrained in the water alongside the stern of the boat or secured to a partially submerged platform. Because tiger sharks are obligate ram ventilators, a hose was then placed in the mouth to pump water over the gills. Pre-caudal length (PCL), a standard metric of shark body length, was measured on all sharks following standard protocols. The sharks were stretched out carefully either on the platform noted above, or alongside the platform, and a flexible tape measure was used to measure the length between the tip of the nose to the insertion of the caudal fin (PCL). Every effort was made to avoid the

sharks being bent, which would increase measurement error. All sharks were sampled at various locations of Southern Florida and the Northern Bahamas, which included the following areas: throughout the middle Florida Keys (USA), namely Biscayne Bay, Florida Bay and the reefs off Islamorada, Florida. Further, we performed additional sampling around Grand Bahama, Bahamas. We obtained head data for 18 sharks, and caudal fin data for 16 sharks. The same set of measures was not always possible for every individual due to contingencies such as releasing the shark to maintain health or if parts of the tail were injured or missing. All sharks used for our data were captured between July 2012 and May 2015. This work was done in accordance with an approved animal care and use protocol (IACUC 12-280 to Neil Hammerschlag at the University of Miami).

Images Captured

We used several different handheld digital cameras over the course of the three-year period to obtain lateral images of the caudal fin (Fig. 1). One person would hold the caudal fin by both the caudal peduncle (to support the fin) and by the tip of the upper lobe, so that the fin was parallel to the camera. The fin was kept in a straight (unbent) position to avoid any conformational changes that might result in measurement error. The individual holding the fin would also hold a short ruler (15.24 cm) parallel to the fin to provide a scale bar. The images were taken parallel to the fin to limit parallax. The same procedure was followed for the head, as images were taken from a dorsal view and parallel to the top of the head, with a ruler placed on the top of the head (Fig. 1).

Elliptical Fourier analysis, calculation of areas, and statistical analyses. We used the magnetic lasso tool and fill layer option in Adobe Photoshop CS6 on a PC to digitally isolate grayscale silhouettes of the caudal fins and heads for the EFA. For the caudal fin, we used the insertion point of the caudal fin on both dorsal and ventral sides and then drew a straight line between these points as the cutoff point for the caudal fin (Fig 1). For the head, we used the anterior position of the eyes, which can be seen from above (Fig. 1) as the landmarks for the head, and drew a straight line between these points. Our method does not take into account the complex curvature and anatomy of the lower jaw of tiger sharks, but as the top of the head in tiger sharks is generally relatively flat compared to other sharks, these digital head cut-outs are representative of key aspects of head shape, especially head width, and the degree to which the head becomes more rounded. EFA takes the outline of closed two-dimensional silhouettes and maps the distance from a specified origin to each point on the outline to create a polar coordinate function, which can be expressed with a set of harmonics, with numbers ranging from one to infinity. The lower harmonics roughly describe features of outlines while the higher harmonics capture more subtle variation; so using a greater number of harmonics allows us to capture increased subtle variation in shape. These harmonic coefficients can then be condensed into a set of principal component analysis (PCA, Lestrel, 2008). We therefore used PCA to condense the information into three PCs (for caudal fins, which accounted for 93% of total variation) and two principal components (PCs, for heads, which accounted for 95% of total variation) principal components.

To calculate the areas of the caudal fin and head, we used the freehand selections tool in ImageJ (Rasband, 1997−2014) to obtain area measurements of heads and fins. Head and caudal fin areas were calculated from digital cut-outs used for the Elliptical Fourier analyses. Finally, we measured head length as the distance from the middle of the line connecting the eyes to the tip of the snout (Fig. 1). PCL, the linear distance between the tip of the snout to the insertion of the caudal fin, was our scaling metric (following Irschick and Hammerschlag, 2014).

All statistics were performed using Minitab 17 on a PC laptop (Minitab 17 Statistical Software (2010). [Computer software]. State College, PA: Minitab, Inc. (www.minitab.com)). To calculate scaling coefficients, we regressed head and caudal fin

Variable	Slope	RMA slope	y-int	F	df	P	R^2	T-value	P-value (t-test)
Caudal fin area	1.76 + 0.13	1.83	−1.12 + 0.31	166.4	2,13	<0.001	0.93	1.30	>0.40
Head area	1.18 ± 0.35	1.82	−0.27 ± 0.80	11.6	2,16	0.0037	0.42	0.51	>0.50
Head length	0.76 ± 0.11	0.88	−0.58 ± 0.26	47.2	2,16	<0.001	0.75	1.09	>0.40

The primary statistics (*F*-values, *P*-values) are from linear least-squares regressions, but RMA regression slopes are also provided to correct for error in the independent variable. The *t*-values are from *t*-tests comparing the actual slope versus an expected slope using the RMA slopes.

area, as well as head length (in separate regressions) against PCL values using linear least-squares regression, which generated the statistics (e.g., F-values) shown in Table 1. All variables were log-transformed prior to calculating regressions. Because the interpretation of scaling coefficients is controversial and often a point of confusion (Smith, 2009), we opted to use reduced major axis regression (RMA) slopes to compare against the hypothesized isometric values (expected slope of 2 for an area versus length, and 1 for a length versus a length). The RMA slope is the linear least-squares slope divided by the correlation coefficient. We then used standardized *t*-tests to test the predictions versus actual RMA slopes. In addition, we ran regressions on plots of PCL vs. head and caudal fin shape,

respectively. We used the standard criterion of $P<0.05$ as our metric of statistical significance.

RESULTS

Both caudal fin area and head area showed a positive relationship with PCL (Table 1, Fig. 2). Caudal fin area did not scale significantly different from the expected isometric value of 2 (Table 1, Fig. 2), even though the degree of variability in this trait was far less than for head area. Head area also showed no substantial deviation from the expected isometric slope of 2 (Table 1). Finally,
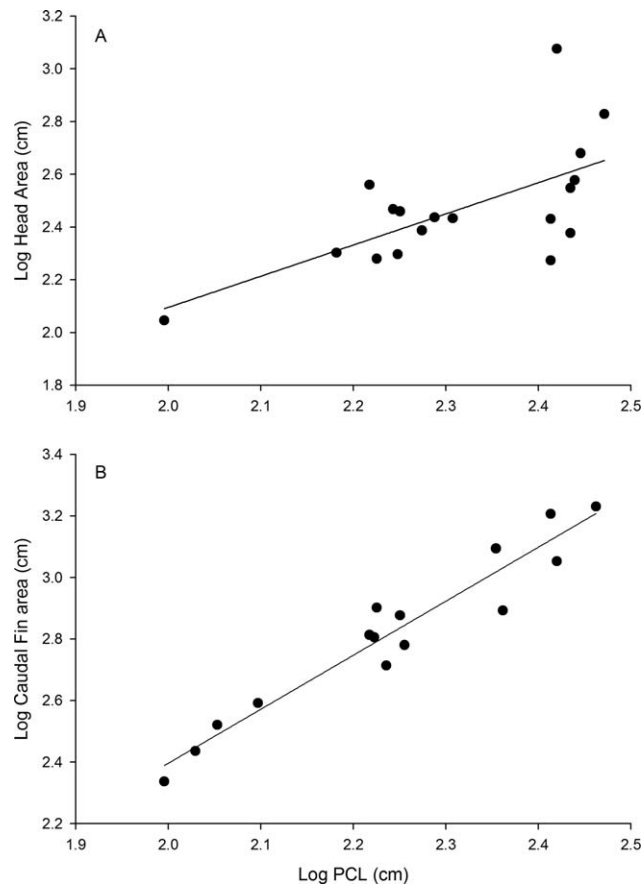

Fig. 2. (A) A plot of log-transformed values of pre-caudal length (x-axis) versus log-transformed caudal fin area (y-axis). (B) A plot of log-transformed values of PCL (x-axis) versus log-transformed head area (y-axis). Pre-caudal length (cm).

TABLE 2. *Results from PCA of seven harmonics from EFA that described caudal fin shape among a sample of tiger sharks*

	PC1	PC2	PC3	PC4
Eigenvalue	0.006	0.004	0.002	0.0004
% variation explained	47	30	16	3
A1	<0.0001	<0.0001	<0.0001	<0.0001
A2	−0.2032	−0.1450	0.3098	−0.4621
A3	−0.0750	−0.0253	−0.0024	−0.2773
A4	0.0193	0.0151	0.1125	−0.1857
A5	0.0224	0.0316	0.0147	0.0271
A6	0.0162	−0.0119	0.0435	0.0870
A7	−0.0264	−0.0317	−0.0232	0.1521
B1	<0.0001	<0.0001	<0.0001	<0.0001
B2	0.0555	0.3493	0.3518	0.1928
B3	0.1036	0.2493	0.1948	0.1565
B4	−0.0107	0.2315	0.2464	0.2532
B5	−0.0418	0.0470	0.1109	0.1437
B6	−0.0633	−0.0038	0.0710	0.0743
B7	−0.0190	−0.0696	−0.0251	−0.0180
C1	<0.0001	<0.0001	<0.0001	<0.0001
C2	−0.7684	0.4708	−0.3747	−0.0781
C3	0.0185	0.3926	0.4663	−0.4058
C4	0.0899	0.1794	−0.1519	−0.0962
C5	0.1854	0.0748	0.0547	−0.1340
C6	0.0230	−0.0414	−0.1468	0.2483
C7	−0.0126	−0.0337	0.0047	0.1085
D1	0.4579	0.2343	−0.4658	−0.3967
D2	0.2271	0.4076	−0.1202	0.1582
D3	0.1280	0.1976	−0.0510	0.0656
D4	−0.0166	0.0712	0.0235	0.1433
D5	−0.0899	−0.1043	0.0811	0.0296
D6	−0.1049	−0.1344	0.0391	0.0524
D7	−0.0156	−0.1437	0.0128	−0.0954

Because each EFA harmonic had four coefficients (A, B, C, and D), there were 28 variables in the PCA.

TABLE 3. *Results from PCA of seven harmonics from EFA that described head shape among a sample of tiger sharks*

	PC1	PC2	PC3	PC4
Eigenvalue	0.0025	0.0007	0.00009	0.00003
% variation explained	75	20	3	1
A1	<0.0001	0	<0.0001	<0.0001
A2	0.0442	−0.3452	−0.0859	0.4403
A3	0.2218	0.0409	0.0896	0.0009
A4	0.0297	−0.3038	−0.0444	0.2036
A5	0.0997	0.0248	0.1200	0.0422
A6	0.0040	−0.0817	−0.0061	0.1125
A7	0.0290	0.0226	−0.0195	0.0089
B1	<0.0001	<0.0001	<0.0001	<0.0001
B2	0.1150	0.0181	−0.3902	−0.5425
B3	−0.0037	0.2124	−0.0370	0.1608
B4	0.0028	0.0167	−0.1900	0.0229
B5	−0.0046	0.1397	−0.0326	0.1440
B6	−0.0753	0.0123	−0.0673	0.0816
B7	−0.0176	0.1485	−0.0005	0.0464
C1	<0.0001	<0.0001	<0.0001	<0.0001
C2	0.0584	0.0605	−0.6687	0.3857
C3	−0.0100	0.1643	−0.0317	0.2554
C4	−0.1400	0.0171	0.1117	0.3354
C5	−0.0089	0.1117	−0.0136	0.0228
C6	−0.0477	0.0064	−0.1117	0.0143
C7	−0.0093	0.0892	0.0298	0.0597
D1	−0.9413	−0.0712	−0.0663	−0.0845
D2	−0.0603	0.7790	0.0289	0.0852
D3	−0.0006	0.0219	−0.5317	−0.1452
D4	−0.0005	0.1071	−0.0097	0.1393
D5	0.0087	−0.0084	0.0906	−0.0101
D6	0.0149	−0.1276	−0.0262	−0.0429
D7	0.0479	−0.0030	0.0365	−0.1112

Because each EFA harmonic had four coefficients (A, B, C, and D), there were 28 variables in the PCA.
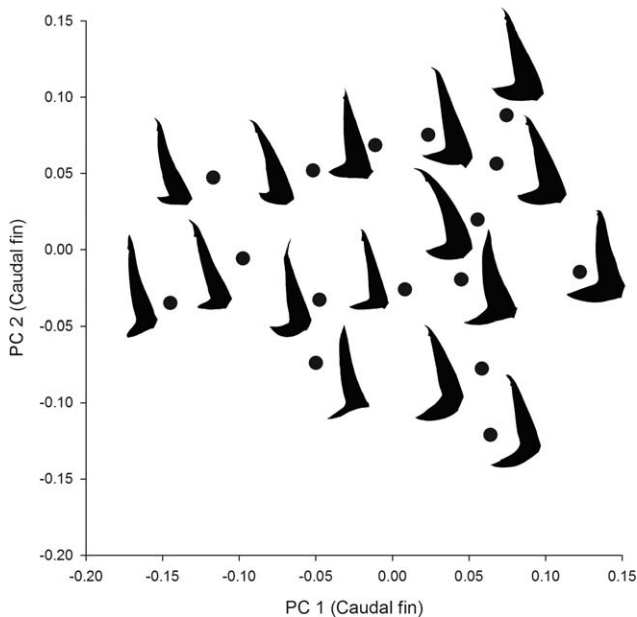

Fig. 3. A plot of PC 1 (x-axis) versus PC 2 (y-axis) from the PCA on caudal fin shape based on the EFA. Silhouettes of caudal fins are included next to a variety of points to demonstrate the range of caudal fin shapes among the tiger sharks sampled.
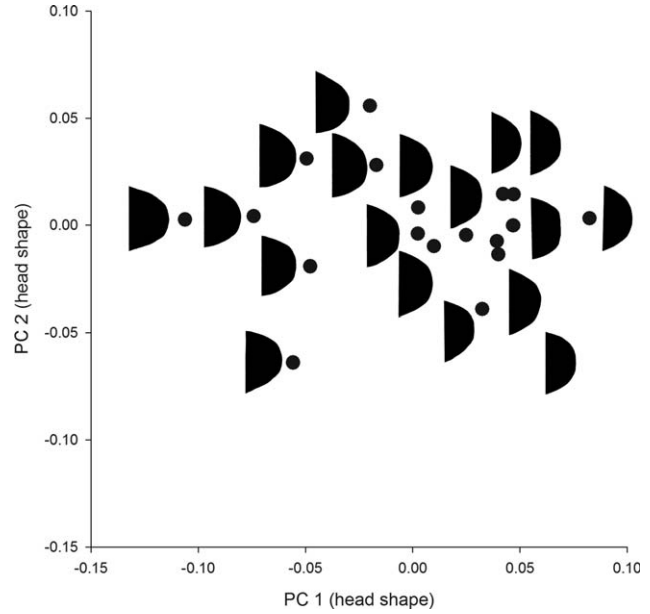
Fig. 4. A plot of PC 1 (x-axis) versus PC 2 (y-axis) from the PCA on head shape based on the EFA. Silhouettes of heads are included next to a variety of points to demonstrate the range of head shapes among the tiger sharks sampled.

head length also showed a positive relationship with PCL, with no significant deviation from the expected isometric slope of 1 (Table 1).

Tables 2 and 3 provide loadings for the harmonics from the EFA for the caudal fin and head shape, respectively. The harmonics cannot easily be understood or compared to traditional linear morphological variables such as head length, and as noted by other authors, the best method for interpretation is through visualization. Therefore, Figures 3 and 4 provide plots of PCs 1 and 2 for the multivariate analysis of the harmonics for caudal fin shape and head shape, respectively. Alongside each point is the corresponding silhouette for caudal fins and heads for that individual. For the caudal fins (Fig. 3), the first two PCs explain 47% and 30% of the total shape variation (77% total, Table 2). The first PC describes an axis of relative symmetry of the upper and lower lobes, in which individuals with high values of PC 1 have more symmetrical lobes, whereas individuals with low values of PC 1 have more asymmetrical lobes, with the lower lobe being substantially smaller than the upper lobe. The second PC exhibits less variation and is more challenging to interpret, but appears to reflect variation in the aspect ratio of the fins, with individuals with high values having shorter but wider fins, and individuals with low values have higher and narrower fins.

For head shape (Fig. 4), the first two PCs explain 75% and 20% of the total shape variation (95% total, Table 3). The first PC appears to describe an
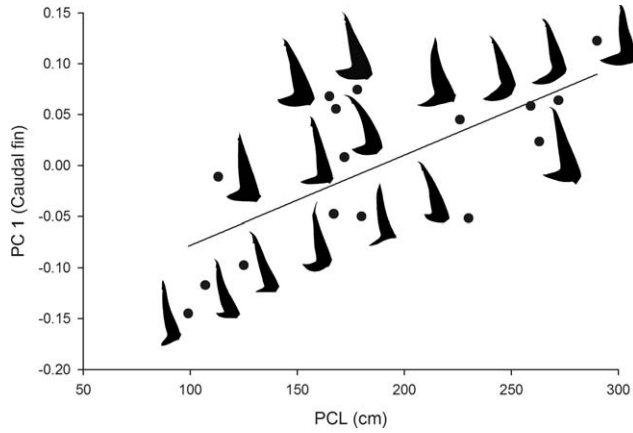
Fig. 5. Values of pre-caudal length (x-axis) versus PC 1 (y-axis) for caudal fin shape. Each value represents an individual shark. The silhouettes of caudal fins are from individual sharks. Note the transition from relatively asymmetrical tails as juveniles to more symmetrical tails as adults.
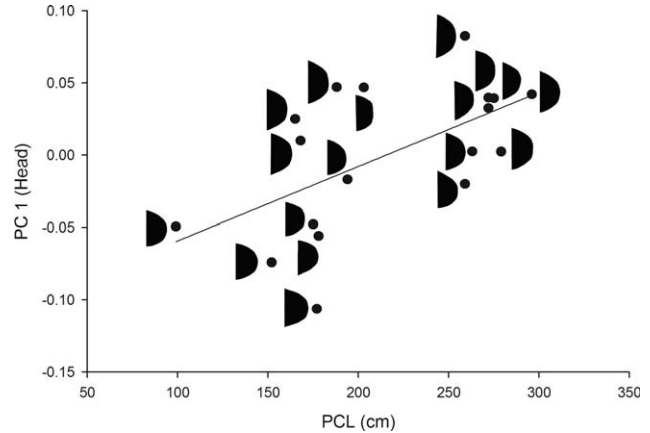

Fig. 7. Values of pre-caudal length (x-axis) versus PC 1 (y-axis) for head shape. Each value represents an individual shark. The silhouettes of heads are from individual sharks. Note the transition from relatively conical heads as juveniles to wide blunt heads as adults.

axis of relative elongation, with individuals with large values having relatively wide, blunt heads, and individuals with small values having more elongate, rounded heads, although the overall difference does not appear to be substantial. The second PC, as with the caudal fins, exhibits far less variation, and appears to present no clear variation in shape among different individuals.

The values for PC 1 for the caudal fin were positively correlated with PCL ($r^2=0.50$, $F_{1,13}=13.7$, $P<0.005$), revealing a proportional change in shape. In juvenile tiger sharks, the lower lobe of the caudal fin was relatively shorter in relation to the upper lobe, leading to more asymmetrical fins (Fig. 5). As tiger sharks mature, the upper and lower lobes of the caudal fins become gradually more symmetrical, resulting in adults with far more symmetrical fins compared to juveniles (Figs. 5 and 6). Pre-caudal length showed no significant relationship with either PC 2 ($r^2=0.08$, $F_{1,14}-1.29$, $P>0.30$), or PC 3 ($r^2=0.002$, $F_{1,14=0.03}$, $P>0.75$) for caudal fin shape. There was a positive relationship between PC 1 for head shape versus PCL ($r^2=0.33$, $F_{2,16}=8.0$, $P<0.025$, Fig. 7). In juvenile
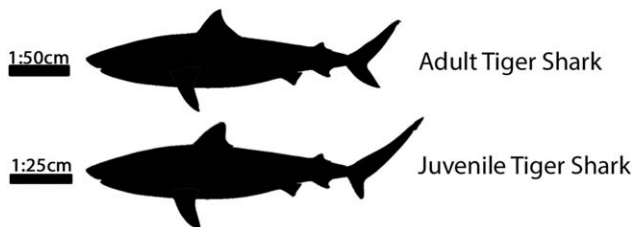

Fig. 6. Representative tiger shark silhouettes showing the proportional change in caudal fin area with size. The fins on the silhouette are digital cut-outs taken from actual sharks.

tiger sharks, the head is more rounded anteriorly, and is less wide, and gradually transitions to a wider and blunter shape in adults, although the overall degree of shape change seems less dramatic compared to the caudal fin. However, PCL showed no significant relationship with PC 2 ($r^2=0.001$, $F_{1,16}=0.01$, $P>0.75$) for head shape. As additional PCs beyond the first one for both caudal fin shape and head shape head shape did not show significant relationships with body size, therefore we do not discuss this further.

DISCUSSION

Our analysis reveals that caudal fin area, head area, and head length, each scaled isometrically as tiger sharks grow, and both caudal fin and head shape change systematically with size in tiger sharks. Juvenile tiger sharks have relatively asymmetrical caudal fins in which the lower lobe is smaller than the upper lobe, whereas adults display a more symmetrical design. Juvenile tiger sharks display a more conical nose, whereas adults present a broader blunter nose in dorsal view.

Functional and ecological data are both essential for interpreting changes in body form among and within species (Hildebrand et al., 1985; Ricklefs and Miles 1994; Lauder and Reilly, 1996; Irschick and Kuo, 2012). While we lack functional data on how the caudal fin is employed in tiger sharks, prior experimental and theoretical data (Alexander, 1965; Webb, 1984; Lauder, 1989; Ferry and Lauder, 1996; Liao and Lauder, 2000; Lauder, 2000; Wilga and Lauder, 2002; Lauder et al., 2003; Blake, 2004) provides some context. Shark species differ in the underlying structure and degree of symmetry of the caudal fin, such as contrasting the more symmetrical caudal fin shape of white

and mako sharks (Donley et al., 2004; Wilga and Lauder, 2004a; Lingham-Soliar, 2005a,b; see also Montani, 2002) versus the less symmetrical caudal fin shape of slow cruisers such as nurse sharks or cow sharks (Thomson and Simanek, 1977; Wilga and Lauder, 2004a). Some fish species with heterocercal tails (e.g., leopard sharks (*Triakis semifasciata*), bamboo sharks (*Chiloscyllium plagiosum*), and spiny dogfish (*Squalus acanthias*) show that they, and sturgeon (Acipenseridae) tend to swim at a slight upward angle to the flow to offset the asymmetrical caudal fin's reactionary force that tends to push the head downwards, resulting in the shark moving horizontally without change in vertical position (Ferry and Lauder, 1996; Wilga and Lauder 2004a, 2004a; Flammang et al., 2011). Fluid dynamics could be used to compare the wake of juvenile vs adult tiger shark tail models to test for functional differences that may be attributed to shape differences if live animals could be studied in a controlled laboratory setting. Furthermore, experiments with simple robotic models of different tail shapes has shown that tail shape can influence swimming speed, and that there is a tradeoff between speed and cost of transport (Lauder et al., 2011, 2012). Based on these data, the more heterocercal shape in juveniles may allow somewhat greater relative swimming speeds, but at increased cost of transport relative to the more symmetrical shape in adults. The more symmetrical tail shape in adults might also increase the lift to drag ratio and perhaps change the angle of thrust.

Tracking data is revealing behavioral difference between juvenile and adult tiger sharks in their propensity to make long-distance migrations (Meyer et al., 2009; Hammerschlag et al., 2012; Papastamatiou et al., 2013). Adult tiger sharks will regularly migrate thousands of kilometers, often moving at relatively high rates of speed (e.g., Holland et al., 1999, Papastamatiou et al., 2013, Ferriera et al., 2015, Hammerschlag et al., 2012). While more comparative tracking data on juvenile tiger sharks is needed, available information suggest that their movement patterns are more confined (Meyer et al., 2009; Werry et al., 2014, Alfonso and Hazin, 2015, Lea et al., 2015). Prior research shows that young sharks often have higher site-fidelity or smaller home range compared to adults, perhaps due to the threat of predation, lack of experience, or energetic and physiological constraints (see Speed et al., 2010). Thus, one possible explanation for this ontogenetic shift is that the more symmetrical fin of adult tiger sharks is better suited for long-distance migrations, which are often undertaken at relatively high rates of movement (for example, mean swimming speeds of 3.85 km/h in Holland et al., 1999, dispersion rates of up to 50 km/day in Hammerschlag et al. 2012) and the more asymmetrical fin of juvenile tiger sharks is better suited for an active lifestyle of catching fish, and for moving within relatively smaller home ranges. While laboratory functional studies with tiger sharks would be challenging, field studies examining rates of movement in tiger sharks of varying sizes, as well as modeling locomotion, perhaps using 3D-printed models in flow-tanks, would be valuable in understanding these patterns.

Head shape in vertebrates is closely linked to diet (Motta, 2004; Alfaro et al., 2005; Dean et al., 2007a,b), and prior work has shown variation among shark species in teeth and jaw morphology (Huber and Motta, 2004, Huber et al., 2005, 2006, 2008, 2009; Lowry et al., 2007; Ramsay and Wilga, 2007; Whitenack and Motta, 2010). Sharks that eat larger prey (e.g., white sharks, bull sharks, tiger sharks) present triangular blade-like teeth designed for shearing off chunks of tough muscle and bone (Frazzetta, 1988; Huber et al., 2009; Whitenack and Motta, 2010; Habegger et al., 2012). Sharks that specialize on smaller fish typically present dagger-like teeth designed for grabbing slippery prey that are consumed whole, and smaller heads and gapes. Our data show that on the one hand, juveniles have relatively larger heads than adults, but also that their heads are more conical. Various head size metrics scale with negative allometry in leopard sharks and blacktip sharks (Lowry et al., 2007; Irschick and Hammerschlag, 2014), and with isometry in larger bull and nurse sharks. The relatively wide blunt heads of tiger sharks is consistent with other data indicating that broad heads can increase bite force by allowing greater attachment area for muscles (Meyers et al., 2002; Huber et al., 2009), and this may allow adult tiger sharks to more effectively shear through larger and harder prey they consume as adults (i.e., turtles, mammals).

Previous work (Frazetta, 1988[AQ]; Whitenack and Motta, 2010; Habegger et al., 2012) shows that the teeth structure of sharks is correlated with bite force, and their ability to shear through hard prey. As noted by Whitenack and Motta (2010), tiger shark teeth are designed for shearing hard prey such as turtle shells, and that a large bite circumference would facilitate this behavior, so there is a clear interaction between head shape and tooth shape. Studies relating tooth shape and head shape in adult versus juvenile tiger sharks would therefore be interesting, especially given documented changes in biting performance across ontogeny in other sharks (e.g., blacktip sharks, Huber et al. 2009). In conclusion, we have demonstrated changes in caudal fin shape and head shape across ontogeny in a predatory shark. Our work sheds light on how ontogenetic changes in morphology could potentially impact the ecology of a key predator in tropical seas.

ACKNOWLEDGMENTS

LITERATURE CITED

Alexander RMN. 1965. The lift produced by the heterocercal tails of Selachii. J Exp Biol 43:131–138.

Alfaro ME, Bolnick DI, Wainwright PC. 2005. Evolutionary consequences of many-to-one mapping of jaw morphology to mechanics in labrid fishes. Am Nat 165:E140–E154.

Alfonso SA, Hazin FH. 2015. Vertical movement patterns and ontogenetic niche expansion in tiger shark, *Galeocerdo cuvier*. PLoS One 10:e01116720. (doi: 10.1371/journal.pone.0116720).

Beck MW, Heck KL Jr, Able KW, Childers DL, Eggleston DB, Gillanders BM, Halpern B, Hays CG, Hoshino K, Minello TJ, Orth RJ, Sheridan PF, Weinstein MP. 2001. The identification, conservation and management of estuarine and marine nurseries for fish and invertebrates. Bioscience 51:633–641.

Blake RW. 2004. Fish functional design and swimming performance. J Fish Biol 65:1193–1222.

Calder WA. 1984. Size, Function and Life History. Massachusetts: Harvard University Press. 431 p

Carrier D. 1996. Ontogenetic limits on locomotor performance. Phys Zool 69:467–488.

Casey JC, Pratt HL Jr, Stillwell CE. 1985. Age and growth of the sandbar shark (*Carcharhinus plumbeus*) from the western North Atlantic. Can J Fish Aquat Sci 42:963–975.

Casey JG, Natanson LJ. 1992. Revised estimates of age and growth of the sandbar shark (*Carcharhinus plumbeus*) from the western North Atlantic. Can J Fish Aquat Sci 49:1474–1477.

Compagno LJV, Dando M, Fowler S. 2005. A Field Guide to the Sharks of the World. London, UK: Harper Collins. 496 p.

Cortes E. 1999. Standardized diet compositions and trophic levels of sharks. ICES J. Mar Sci 56:707–717.

Dean MN, Azizi E, Summers AP. 2007a. Uniform strain in broad muscles: morphological innovation in the jaw adductor of the chimaera, *Hydrolagus colliei*. J Exp Biol 210:3395–3406.

Dean MN, Bizzaro JJ, Summers AP. 2007b. The evolution of cranial design, diet and feeding mechanisms in batoid fishes. Integr Comp Biol 47:70–81.

Donley JM, Sepulveda CA, Konstantinidis P, Gemballa S, Shadwick RE. 2004. Convergent evolution in mechanical design of lamnid sharks and tunas. Nature 429:61–65.

Eggold BT, Motta PJ. 1992. Ontogenetic dietary shift and morphological correlates in striped mullet, *Mugil cephalus* L. Env Biol Fishes 34:139–158.

Estes JA, Terborgh J, Brashares JS, Power ME, Berger J, Bond WJ, Carpenter SR, Essington TE, Hold RD, Jackson JB, Marquis RJ, Oksanen L, Oksanen T, Paine RT, Pikitch EK, Ripple WJ, Sandin SA, Scheffer M, Schoener TW, Shurin JB, Sinclair AR, Soule ME, Virtanen R, Wardle DA. 2011. Trophic downgrading of planet Earth. Science 333:301–306.

Ferriera LC, Thums M, Meeuwig JJ, Vianna FM, Stevens J, McAuley R, Meekan MG. 2015. Crossing Lattitudes-long distance tracking of an apex predator. PLos One 10:e0116916. doi: 10.1371/journal.pone.0116916)

Ferry L, Lauder G. 1996. Heterocercal tail function in leopard sharks: A three-dimensional kinematic analysis of two models. J Exp Biol 199:2253–2268.

Fitzpatrick R, Thums M, Bell I, Meekan MG, Stevens JD, Barnett A. 2012. A comparison of the seasonal movements of tiger sharks and green turtles provides insight into their predator-prey relationship. PLoS One 7:e51927

Flammang BE, Lauder GV, Troolin DR, Strand T. 2011. Volumetric imaging of shark tail hydrodynamics reveals a three-dimensional dual-ring vortex wake structure. Proc R Soc Lond B 278:3670–3678.

Frazzetta TH. 1988. The mechanics of cutting and the form of shark teeth (Chondrichthyes, Elasmobranchii). Zoomorphology 108:93–107.

Gallagher AJ, Wagner DN, Irschick DJ, Hammerschlag N. 2014. Body condition predicts energy stores in apex predatory sharks. Cons Phys 2:cou022 DOI: 10.1093/conphys/

Habegger ML, Motta PJ, Huber DR, Dean MN. 2012. Feeding biomechanics and theoretical calculations of bite force in bull sharks (*Carcharhinus leucas*) during ontogeny. Zoology 115:354–364.

Hammerschlag N, Gallagher AJ, Wester J, Luo J, Ault JS. 2012. Don't bite the hand that feeds: assessing ecological impacts of provisioning ecotourism on an apex marine predator. Func Ecol 26:567–576.

Heithaus MR. 2001. The biology of tiger sharks, *Galeocerdo cuvier*, in Shark Bay, Western Australia: Sex ratio, size distribution, diet, and seasonal changes in catch rates. Env Biol Fishes 61:25–36.

Heithaus MR, Wirsing AJ, Dill LM, Heithaus LI. 2007. Long-term movements of tiger sharks satellite-tagged in Shark Bay, Western Australia. Mar Biol 151:1455.

Herrel A, Van Damme R, De Vree F. 1996. Sexual dimorphism of head size in *Podarcis hispanica atrata*: Testing the dietary divergence hypothesis by bite force analysis. Netherlands. J Zool 46:253–262.

Herrel A, Vanhooydonck B, Joachim R, Irschick DJ. 2004. Frugivory in polychrotid lizards: Effects of body size. Oecologia 140:160–168.

Hildebrand M, Bramble DM, Liem KF, Wake DB. 1985. Functional Vertebrate Morphology. Massachusetts: Belknap Press. 430 p.

Holland KN, Weatherbee BM, Lowe CG, Meyer CG. 1999. Movements of tiger sharks (Galeocerdo cuvier) in coastal Hawaiian waters. Mar Biol 134:665–673.

Huber DR, Motta PJ. 2004. Comparative analysis of methods for determining bite force in the spiny dogfish *Squalus acanthias*. J Exp Zool 301:26–37.

Huber DR, Eason TG, Hueter RE, Motta PJ. 2005. Analysis of the bite force and mechanical design of the feeding mechanism of the durophagous horn shark *Heterodontus francisci*. J Exp Biol 208:3553–3571.

Huber DR, Weggelaar CL, Motta PJ. 2006. Scaling of bite force in the blacktip shark *Carcharhinus limbatus*. Zoology 109:109–119.

Huber DR, Dean MN, Summers AP. 2008. Hard prey, soft jaws and the ontogeny of feeding mechanics in the spotted ratfish *Hydrolagus colliei*. J R Soc Int 5:941–952.

Huber DR, Claes JM, Mallefet J, Herrel A. 2009. Is extreme bite performance associated with extreme morphologies in sharks? Phys Biochem Zool 82:20–28.

Irschick DJ, Hammerschlag N. 2014. Morphological scaling of body form in four shark species differing in ecology and life history. Biol J Linn Soc 114:126–135.

Irschick DJ, Kuo C. 2012. Functional traits of species and individuals. In: Hastings A, Gross L, editors. Sourcebook in Theoretical Ecology. California: University of California Press. pp. 324–329.

LaBarbera M. 1989. Analyzing body size as a factor in ecology and evolution. Ann Rev Ecol Syst 20:97–117.

Lauder GV. 1989. Caudal fin locomotion in rayfinned fishes: Historical and functional analyses. Amer Zool 29:85–102.

Lauder GV. 1996. The argument from design. In: Rose MR, Lauder GV, editors. Adaptation. California: Academic Press. pp. 55–91.

Lauder GV. 2000. Function of the caudal Fin during locomotion in fishes: kinematics, flow visualization, and evolutionary patterns. Int Comp Biol 40:101–122.

Lauder GV. Reilly SM. 1996. The mechanistic bases of behavioral evolution: a multivariate analysis of musculoskeletal function. In Martins E, editor. Phylogenies and the Comparative Method in Animal Behavior. Massachusetts: Oxford University Press. pp. 104–137.

Lauder GV, Drucker EG, Nauen J, Wilga CD. 2003. Experimental hydrodynamics and evolution: caudal fin locomotion in fishes. In: Bels VL, Casinos A, Gasc JP, editors. Vertebrate Biomechanics and Evolution I: Theory and Aquatic Animals. Oxford: BIOS Scientific Publishers Ltd. pp. 117–135.

Lauder GV, Lim J, Shelton R, Witt C, Anderson EJ, Tangorra J. 2011. Robotic models for studying undulatory locomotion in fishes. Marine Tech Soc J 45:41–55.

Lauder GV, Flammang BE, Alben S. 2012. Passive robotic models of propulsion by the bodies and caudal fins of fish. Int Comp Biol 52:576–587.

Lea JSE, Wetherbee BM, Queiroz N, Burnie N, Aming C, Sousa LL, Mucientes GR, Humphries NE, Harvey GM, Sims DW, Shivji MS. 2015. Repeated, long-distance migrations by a philopatric predator targeting highly contrasting ecosystems. Nat Sci Rep 5:11202 Article number. doi:10.1038/srep11202

Lestrel PE, editor. 2008. Fourier Descriptors and Their Applications in Biology. Massachusetts: Cambridge University Press. 484 p.

Liao J, Lauder GV. 2000. Function of the heterocercal tail in white sturgeon: flow visualization during steady swimming and vertical maneuvering. J Exp Biol 203:3585–3594.

Lingham-Soliar T. 2005a. Caudal fin allometry in the white shark Carcharodon carcharias: implications for locomotory performance and ecology. J Morphol 92:231–236.

Lingham-Soliar T. 2005b. Caudal fin in the white shark, Carcharodon carcharias (Lamnidae): a dynamic propeller for fast, efficient swimming. J Morphol 264:233–252.

Lowe CG, Wetherbee BM, Crow GL, Tester AL. 1996. Ontogenetic dietary shifts and feeding behavior of the tiger shark Galeocerdo cuvier, in Hawaiian Waters. Env Biol Fishes 47: 203–211.

Lowry D, Motta PJ, Heuter RE. 2007. The ontogeny of feeding behavior and cranial morphology in the leopard shark Triakis semifasciata (Girard 1854): a longitudinal perspective. J Exp Mar Biol Ecol 341:153–167.

Meyer CG, Clark TB, Papastamatiou YP, Whitney NM, Holland KN. 2009. Long-term movements of tiger sharks (Galeocerdo cuvier) in Hawaii. Mar Ecol Prog Ser 381:223–235. doi: 10.3354/meps07951

Meyers JJ, Herrel A, Birch J. 2002. Scaling of morphology, bite force and feeding kinematics in an Iguanian and a scleroglossan lizard. In Aerts P, D'Aout K, Herrel A, Van Damme R, editors. Topics in Functional and Ecological Vertebrate Morphology. Germany: Shaker Publishing. pp. 47–62.

Montani R. 2002. Scaling effects in caudal fin propulsion and the speed of ichthyosaurs. Nature 415:309–312.

Motta PJ. 2004. Prey capture behavior and feeding mechanics of elasmobranchs. In Carrier J, Musick J, Heithaus M, editors. Biology of Sharks and Their Relatives. Florida: CRC Press. pp. 165–202.

Papastamatiou YP, Meyer CG, Carvahlo F, Dale JJ, Hutchinson MR, Holland KN. 2013. Telemetry and random-walk models reveal complex patterns of partial migration in a large marine predator. Ecology 94:2595–2606.

Ramsay JB, Wilga CD. 2007. Morphology and mechanics of the teeth and jaws of white-spotted bamboo sharks (Chiloscyllium plagiosum). J Morphol 268:664–682.

Rasband WS. 1997−2014. ImageJ. Bethesda, MD: U. S. National Institutes of Health. Available at: http://imagej.nih.gov/ij/

Reiss KL, Bonnan MF. 2010. Ontogenetic scaling of caudal fin shape in Squalus acanthias (Chondrichthyes, Elasmobranchii): a geometric morphometric analysis with implications for caudal fin functional morphology. Anat Rec 293:1184–1191.

Ricklefs RE, Miles DB. 1994. Ecological and evolutionary inferences from morphology: An ecological perspective. In Wainwright PC, Reilly SM, editors. Ecological Morphology: Integrative Organismal Biology. Illinois: University of Chicago Press. pp. 13–41.

Schmidt-Nielsen K. 1984. Scaling: Why is Animal Size So Important? Cambridge: Cambridge University Press. 256 p.

Simpfendorfer CA, Goodreid AB, McAuley RB. 2001. Size, sex and geographic variation in the diet of the tiger shark, Galeocerdo cuvier, from Western Australian waters. Env Biol Fishes 61:37–46.

Smith RJ. 2009. Use and misuse of the reduced major axis for line-fitting. Am J Phys Anthropol 140:476–486.

Speed CW, Field IC, Meekan MG, Bradshaw CJA. 2010. Complexities of coastal shark movements and their implications for management. Mar Ecol Prog Ser 408:275–293. doi: 10.3354/meps08581

Thomson KS, Simanek DE. 1977. Body form and locomotion in sharks. Am Zool 17:343–354.

Tyler-Bonner J, Horn HS. 2000. Allometry and natural selection. In: Brown JH, West GB, editors. Scaling in Biology. Oxford, UK: Oxford University Press. pp. 25–35.

Wainwright PC, Osenberg CW, Mittelbach GG. 1991. Trophic polymorphism in the pumpkinseed sunfish (Lepomis gibbosus): Effects of environment on ontogeny. Func Ecol 5:40–55.

Webb PW. 1984. Body Form, locomotion and foraging in aquatic vertebrates. Am Zool 24:107–120.

Werner EE, Gillam JF. 1984. The ontogenetic niche and species interactions in size-structured populations. Ann Rev Ecol Syst 15:393–425.

Werry JM, Planes S, Berumen ML, Lee KA, Braun CD, Clua E. 2014. Reef-fidelity and migration of tiger sharks, Galeocerdo cuvier, across the Coral Sea. Plos One 9:e83249 doi: 10.1371/journal.pone.0083249)

Whitenack LB, Motta PJ. 2010. Performance of shark teeth during puncture and draw: Implications for the mechanics of cutting. 100:271–286

Wilga CD, Lauder GV. 2002. Function of the heterocercal tail in sharks: Quantitative wake dynamics during steady horizontal swimming and vertical maneuvering. J Exp Biol 205: 2365–2374.

Wilga CD, Lauder GV. 2004a. Biomechanics of locomotion in sharks, rays, and chimeras. In Carrier JC, editor. Biology of Sharks and Their Relatives. Florida: CRC Press. pp. 139–164

Wilga CD, Lauder GV. 2004b. Hydrodynamic function of the shark's tail. Nature 430:850

Wirsing AJ, Heithaus MR, Dill LM. 2006. Tiger shark (Galeocerdo cuvier) abundance and growth in a subtropical embayment: Evidence from 7 years of standardized fishing effort. Mar Biol 149:961–968.